B^+ Semileptonic Rare Decays in ATLAS

A. Policicchio
and
G. Crosetti

University of Calabria and INFN Cosenza,
Via P.Bucci, 87036 Arcavacata di Rende, Rende, Italy

ATL-PHYS-PUB-2007-017
16 October 2007

We discuss the latest studies on rare semileptonic decays of B^+ meson with the ATLAS detector.

1. Introduction

Rare B-decays, produced by $b \to s, d$ quark FCNC transitions, are ¡forbidden at the tree level in the Standard Model (SM). These decays occur at the lowest order only through one-loop "penguin" and "box" diagrams. The branching ratios of these decays are very small and they vary between 4×10^{-5} for rare radiative decay $B_d^0 \to K^* \gamma$ down to 10^{-15} for rare Cabibbo suppressed leptonic decay $B_d^0 \to e^+ e^-$.

Rare B-decays careful investigation is mandatory for testing ground of the Standard Model and offer a complementary strategy in the search of new physics by probing the indirect effects of new interactions in higher order processes. The probing of loop-induced couplings provide a means of testing the detailed structure of the SM at the level of radiative corrections. In particular, FCNC involving $b \to s, d$ transitions, provide an excellent probe of new indirect effects of New Physics by yielding informations on the masses and coupling of the virtual particles running in the loops and this explain the attention they have received in recent years. The study of such decays give also other opportunities: to measure the values of $|V_{ts}|$ and $|V_{td}|$ CKM matrix elements and to provide new informations on long-distance QCD effects in matrix elements of the tensor current.

In the last years the B-factories BaBar and Belle presented the first results for $B \to (K^*, K) l^+ l^-$ branching ratios and forward-backward asymmetry (A_{FB}) of these rare semileptonic decays ([1],[2],[3]). The experimental

branching ratio values are consistent with SM predictions even if the statistical errors are very high. More precise measurements are also needed for differential dimuon invariant mass and forward-backward asymmetry distributions, in order to discriminate between SM and New Physics predictions.

The interest in the rare short-distance $FCNC$ contribution to the $B \to l^+l^-K$ decays demands that the mass of the dilepton system should not be compatible with the mass of any hadronic source of dileptons, in particular the J/ψ and the $\psi(2S)$. This out of resonance requirements call for a good mass resolution and thus a good momentum resolution of the two leptons. This cannot be fulfilled with electrons as the energy loss due to Bremsstrahlung is too high. Moreover ATLAS trigger is favourable for dimuon channels, while it's capacity for low P_T dielectron channels is reduced ([8]). Consequently we take into account only dimuon decays.

In this report we will pay our attention to the semileptonic $B^+ \to K^+\mu^+\mu^-$ and $B^+ \to K^{*+}\ \mu^+\mu^-$ decays. We discuss the latest simulation results at ATLAS detector.

2. Theoretical Description

From the theoretical point of view, the $b \to q$ $(q = s, d)$ transitions are described using the effective Hamiltonian

$$\mathcal{H}_{eff} = -4\frac{G_F}{\sqrt{2}}V_{tb}V_{tq}^*\sum_{i=1}^{10}C_i(\mu)O_i(\mu) \tag{1}$$

in the form of Wilson expansion (see e.g. [4]). The set of Wilson coefficients $C_i(\mu)$ depends on the current model and contains the lowest order model contributions and perturbative QCD corrections. The scale parameter μ is approximately equal to the mass of b-quark ($\sim 5GeV$). This parameter separates the perturbative and nonperturbative contributions of the string interactions. The nonperturbative contribution is contained in the matrix elements of basis operators $O_i(\mu)$ between the initial and final hadronic states. For the calculation of these matrix elements it is necessary to use different decay-specific nonperturbative methods: QCD Sum Rules, Heavy Quarks Effective Theory, Quark Models and Lattice calculations. The accuracy in nonperturbative calculations depends on a method, but it is not less than 15%. The accuracy of the Wilson coefficient for with NLO and NNLO QCD corrections ([5]) is not greater than 15% if μ parameter ranges in $[m_b/2, 2m_b]$.

The branching ratios in SM of $B^+ \to K^+\mu^+\mu^-$ and $B^+ \to K^{*+}\ \mu^+\mu^-$ decays can be found in Table 1.

Decay channel	Br. ratio	Ref.	Form Factors	Wilson Coeff.
$B^+ \to K^+\mu^+\mu^-$	3.4×10^{-7}	[6]	QCD LCSR	NNLO
$B^+ \to K^{*+}\ \mu^+\mu^-$	$\sim 10^{-6}$	[6]	QCS LCSR	NNLO

Table 1. *Branching ratios in SM of rare B^+ decays with $\mu^+\mu^-$ pair in final states.*

3. ATLAS Muon Trigger Strategy

At the start up, the target luminosity for the LHC will be $2\times10^{33}cm^{-2}s^{-1}$, rising to the full design luminosity of $10^{34}cm^{-2}s^{-1}$ after few years of running. There will be an average of 4.6 and 23 interactions per bunch crossing for initial and design luminosity respectively. About 1% of collisions will produce a $b\bar{b}$ pair. The challenge for the trigger is to select those events of most interest for the ATLAS B-Physics program ([7]), within the limited trigger and storage resources available. The ATLAS B-Physics trigger ([8],[9],[10]) is based on a muon signature at the first level, which can be accompanied by additional, lower transverse energy signature of leptons and jets. These signatures are refined in the higher trigger levels where specific decays are reconstructed.

For semileptonic dimuon decays, the trigger will be dominated by a dimuon trigger. This is based on the detection of two muons found in the first trigger level with a transverse momentum (p_T) threshold of 6 GeV and 4 GeV respectively. At the second level, the muon p_T measurements will be confirmed in the muon precision chambers, the Tile Calorimeter and then extrapolated to the Inner Detector in order to reject muons from π/K decays. At the Event Filter level, offline track quality reconstruction, vertex and mass cuts will be applied to select candidates for specific exclusive or semi-inclusive decays such as $J/\Psi \to \mu^+\mu^-$ and $B \to \mu^+\mu^-(X)$. This strategy can be used at low initial luminosity and also at nominal LHC $10^{34}cm^{-2}s^{-1}$ luminosity.

4. Signal Data Samples

The data sample for the present studies have been produced in the framework of the DC3 production, using the final ATLAS detector layout, simulation based on Geant4 and new GRID-oriented software ([11], [12], [13]).

The theoretical model for Monte Carlo generation of data samples is shown in Table 1. Pythia ([14]) and Evtgen ([15]) Monte Carlo software packages have been used in the framework of ATLAS software for data production.

The vector meson K^{*+}, has been considered decaying into $K^0_s + \pi^+$

with K_s^0 decaying into two charged pions. The resulting branching ratio for $B^+ \to K^{*+}\ \mu^+\mu^-$ decay with K^{*+}, decaying into $K_s^0 + \pi^+$ and K_s^0 decaying into two charged pions is 4.4×10^{-7}.

At the generation level, the first level trigger cuts have been applied on the first and the second muon ($p_T > 6GeV$ and $p_T > 4GeV$ respectively). Also the Inner Detector acceptance cuts on pseudorapidity and on transverse momentum ($|\eta| < 2.5$ and $p_T > 0.5GeV$) have been applied on stable hadrons.

Quantity	Symbol	Value
Nominal luminosity	$\mathcal{L}$	$10^{33}\ cm^{-2}s^{-1}$
Standard year	t	$10^7\ s$
Annual integrated luminosity	$\mathcal{L} \cdot t$	$10\ fb^{-1}$
$b\bar{b}$ cross section	$\sigma_{b\bar{b}}$	$0.5\ mb$
Generation cut fraction	T	0.01
Probability of $b \to B^+$	P	0.39
Symmetry factor	S	2
$\mathcal{BR}(B \to K^+\mu^+\mu^-)$	$\mathcal{BR}_1$	0.34×10^{-6}
$\mathcal{BR}(B \to K^{*+}\mu^+\mu^-,\ K^{*+} \to K_s^0 + \pi^+,$ $K_s^0 \to \pi^+\pi^-)$	$\mathcal{BR}_2$	0.44×10^{-6}

Table 2. *Relevant assumption for the calculation of the signal yields.*

All numbers used to compute the signal yields are summarized in Table 2. The standard year of running has been assumed $10^7\ s$ at an average luminosity of $\mathcal{L} = 10^{33}\ cm^{-2}s^{-1}$ which corresponds to an integrated luminosity of $10\ fb^{-1}$. The $b\bar{b}$ cross section is considered as an initial assumption which will be revisited after the start of the LHC. The $0.5\ mb$ value ([16]) is a renormalization constant and is thus not affected by errors. The hadronization fraction of the b-quark is taken from the PDG ([17]). The symmetry factor takes into account the charge conjugate decays.

The number of triggerable events expected in 3 years of LHC operation at $\mathcal{L} = 10^{33}\ cm^{-2}s^{-1}$ ($30\ fb^{-1}$ integrated luminosity) has been found $\sim$ 40000 and $\sim$ 51000 for $B \to K^+\mu^+\mu^-$ and $B \to K^{*+}\mu^+\mu^-$ respectively, and it has been calculated as

$$N_i = \mathcal{L} \cdot t \cdot T \cdot S \cdot \sigma_{b\bar{b}} \cdot P \cdot \mathcal{BR}_i \tag{2}$$

Table 3 summarizes the number of simulated events and the number of events expected in $30\ fb^{-1}$ integrated luminosity after cuts at the generation level for each decay channel.

Decay	Triggerable events in 30 fb^{-1}	Simulated events
$B \to K^+\mu^+\mu^-$	~40000	30000
$B \to K^{*+}\mu^+\mu^-$	~51000	50000

Table 3. *Summary table for the $B^+ \to K^+\mu^+\mu^-$ and $B^+ \to K^{*+}\mu^+\mu^-$ (followed by $K^{*+} \to K^0_s\pi^+, K^0_s \to \pi^+\pi^-$) decays. From left, columns contain the decay channel, the number of expected events after cuts at generation level in 30 fb^{-1} and the number of simulated events.*

Below we introduce the basic results of the data analysis. A C++ code has been written in the ATHENA framework for both the decay channels, in order to analyze the AOD reconstruction files ([18], [19]).

5. Signal Reconstruction

5.1. Selection Strategy

The key signature of $B \to \mu\mu K$ events is the presence of the opposite charge muon pair. Due to long B lifetime, this dimuon pair is likely to form a secondary vertex which is detached from the primary vertex. The identification of this vertex, if particularly close to the interaction point, requires leptons which are well reconstructed.

The event selection is done in the following order:

- primary vertex reconstruction; if more than one primary vertex has been reconstructed in the same event, only the one closer to the true vertex is taken into account.
- muon and dimuon selection;
- kaon reconstruction and selection;
- B-meson reconstruction and selection.

Thus the selection has to rely on topological variables as vertex quality and vertex separation requirements. The vertex fitting routine used for this analysis is the CDF vertex fit routine ([20]).

Common requirements for the two decay channels are explained in the following:

- The muon track candidates must fulfill the selection criteria of the muon identification MUID algorithm ([21]).

- The charged track selection for kaon reconstruction is done inside the Inner Detector: the p_T of the track must be above 0.5 GeV and the pseudorapidity $|\eta| < 2.5$. ATLAS cannot identify pions and kaons, therefore all charged particles in the Inner Detector, not identified as muons or electrons, are taken into account.

- Dimuons are formed by two opposite charge muon tracks satisfying the LVL1 trigger ($p_T(\mu_1) > 6\,GeV$, $p_T(\mu_2) > 4\,GeV$ and $|\eta(\mu_1, \mu_2)| < 2.5$) request. They must fulfill the following requirements:

  - the dimuon vertex momentum must not point to primary vertex;
  - the dimuon vertex χ^2/NDF must be lower than 10;
  - the dimuon invariant mass must be in the kinematic allowed window: $2m_\mu < m_{\mu\mu} < m_{B^+} - m_{K^+}$ and $2m_\mu < m_{\mu\mu} < m_{B^+} - m_{K^{*+}}$ respectively for the two decay channels.

5.2. $B^+ \to K^+\mu^+\mu^-$

The $B^+ \to K^+\mu^+\mu^-$ decay is topologically very simple.

After the dimuon selection, a positive charge particle is then searched in the Inner Detector satisfying the charged track selection criteria. For each found dimuon, B^+ candidates are formed using preselected positive charge track. The following final selection criteria are required for the B^+ meson reconstruction:

- the B^+ system must be made of one dimuon and one positive charge track;
- the B^+ vertex χ^2/NDF must be lower than 5;
- the B^+ mass must be in a $\pm 3\sigma$ window around PDG value;
- the B^+ proper time larger than 0.5 ps;
- if more than one B^+ has been reconstructed in the same event, only the one with better χ^2/NDF is taken into account.

The B^+ mass and the B^+ proper time resolution distributions of these accepted events (respectively without cut on B^+ mass and proper time) are shown in Figure 1.

The width of the Gaussian fit for the mass distribution is $\sigma = 42\ MeV$ and 80 fs for the proper time distribution. The B^+ candidate requirements are based on the knowledge of these value.

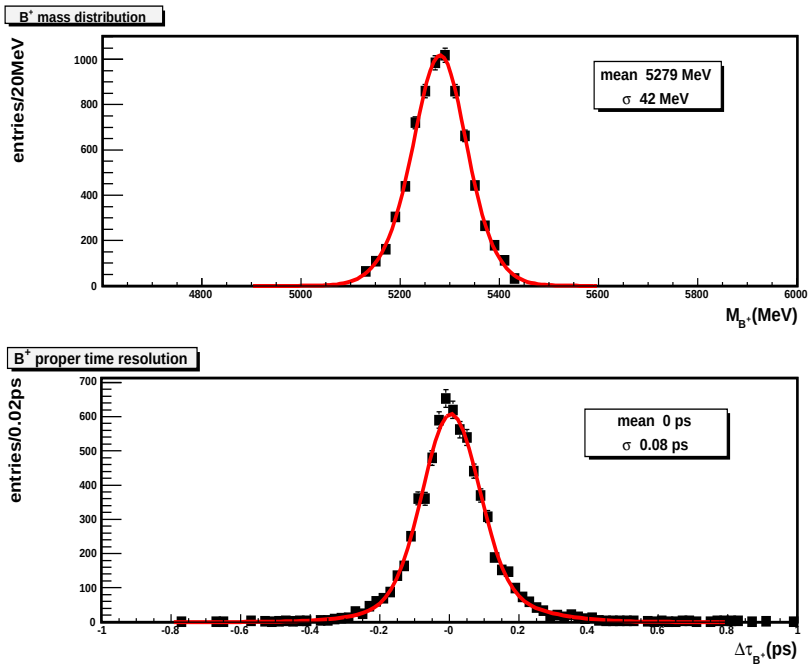

Fig. 1. *B^+ mass and proper time resolution distributions: the mean value and the width of the distribution, resulting from a Gaussian fit, are shown.*

The most interesting distributions for the rare decay channel are the dimuon invariant mass spectrum and the forward-backward asymmetry (FBA). Experimentally this asymmetry is defined as ([22])

$$A_{FB} = \frac{N_F[s_1, s_2] - N_B[s_1, s_2]}{N_F[s_1, s_2] + N_B[s_1, s_2]} \tag{3}$$

where $N_F[s_1, s_2]$ and $N_B[s_1, s_2]$ are the number of positive muons (including the background ones) moving in the forward and backward directions of the B-meson, respectively, in the range of the squared dimuon mass $s\epsilon[s_1, s_2]$.

These two distributions are shown in Figure 2 for true events and reconstructed events. The LVL1 trigger and the analysis cuts do not brought significant changes.

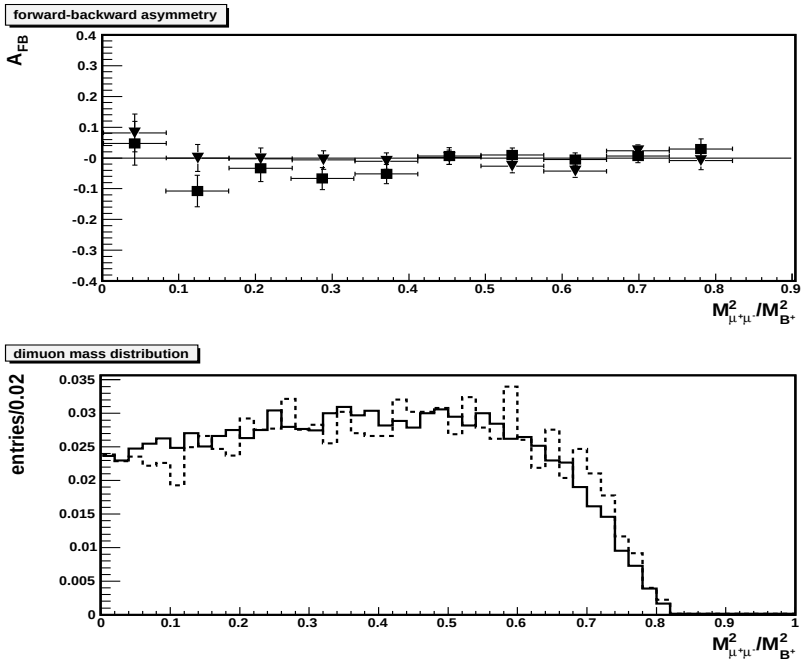

Fig. 2. *$B^+ \to K^+\mu^+\mu^-$ differential FBA and normalized dimuon invariant mass distributions for true (triangles and solid line respectively) and reconstructed (squares and dotted line respectively) events. The horizontal bars in FBA differential distribution represent the dimuon invariant mass bins and the vertical error bars are the statistical errors on FBA.*

5.3. $B^+ \to K^{*+}\mu^+\mu^-$

The $B^+ \to K^{*+}\mu^+\mu^-$ ($K^{*+} \to K^0_s + \pi^+$, $K^0_s \to \pi^+\pi^-$) decay requires a more complex analysis strategy with respect to the $B^+ \to K^+\mu^+\mu^-$ channel due to the reconstruction of the two intermediate particles, K^{*+} and K^0_s.

To reconstruct the K^0_s two opposite charge hadronic tracks are searched in the Inner Detector to be passed at the vertex fit routine. The K^0_s candidates have to fulfill the following requirements:

- the K^0_s momentum have to point to the dimuon vertex;
- the reconstructed K^0_s mass must be in a 3σ mass window around the PDG value;
- the K^0_s vertex χ^2/NDF lower than 10.

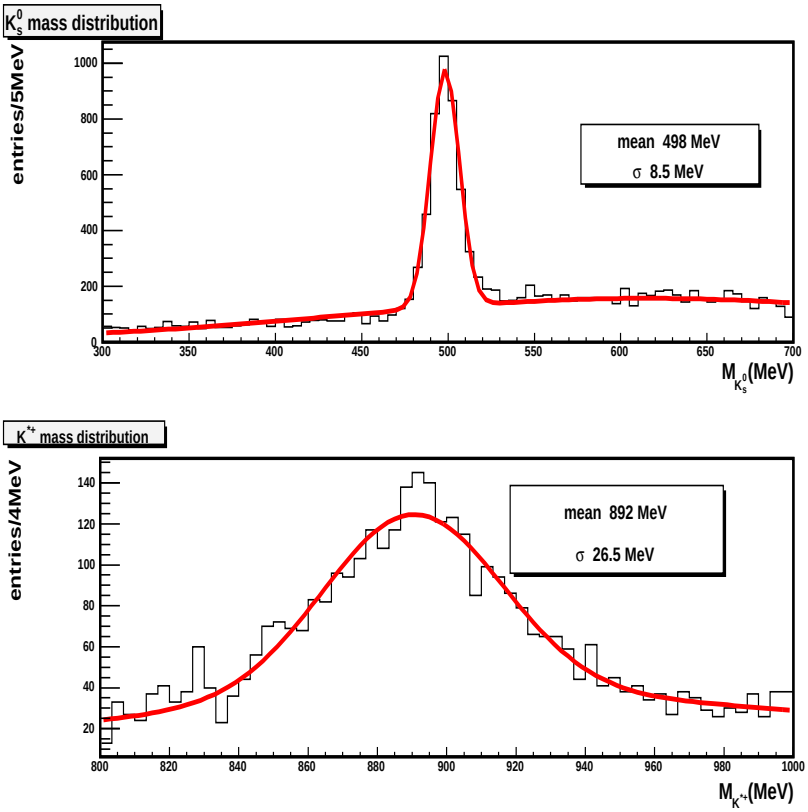

Fig. 3. *Mass distribution for K^0_s and K^{*+} reconstruction: the mean value and the width of the distribution, resulting from a Gaussian fit, are shown.*

The K^0_s mass distribution of events passing these selection criteria (without mass cut) is shown in Figure 3 (top). A Gaussian fit leads to a sigma of 8.5 MeV.

The K^0_s with a third positive charge track coming from dimuon vertex have to form the K^{*+}. The K^{*+} candidates must fulfill the following requirements:

- the K^{*+} vertex χ^2/NDF lower than 5;
- the reconstructed K^{*+} mass must be in a 3σ mass window around the PDG value.

The K^{*+} mass distribution of events passing these selection criteria

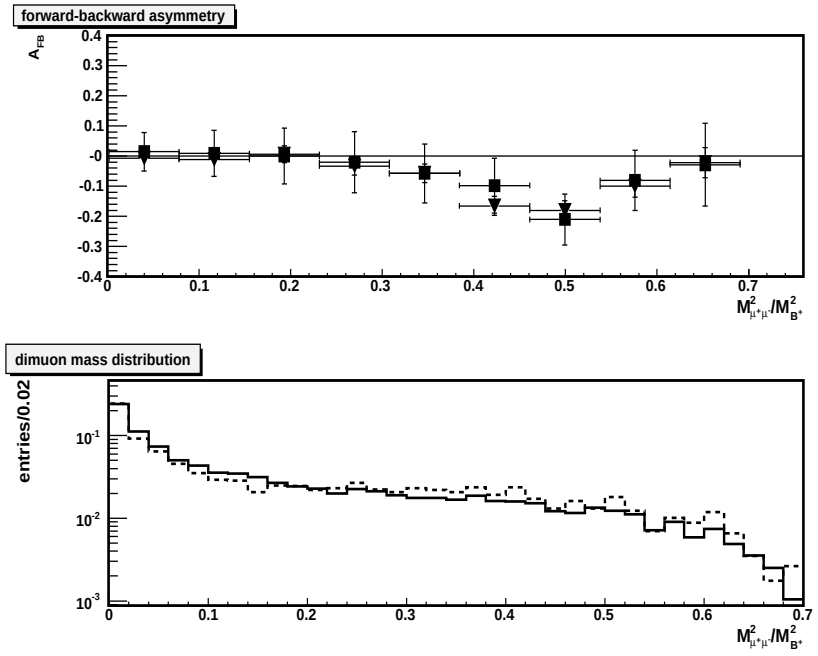

Fig. 4. *$B^+ \to K^{*+}\mu^+\mu^-$ normalized dimuon invariant mass and differential FBA distributions for true (triangles and solid line respectively) and reconstructed (squares and dotted line respectively) events. The horizontal bars in FBA differential distribution represent the dimuon invariant mass bins and the vertical error bars are the statistical errors on FBA.*

(without mass cut) is shown in Figure 3 (bottom). A Gaussian fit leads to a sigma of 26.5 MeV.

For every dimuon, B candidates are formed using preselected kaons. The final selection criteria required for B^+ are the same as those in Subsection 5.2. For this decay the B^+ mass sigma has been found to be 44 MeV.

The dimuon invariant mass and the FBA distributions are shown in Figure 4 both for true data and reconstructed ones. The LVL1 trigger and the reconstruction analysis cuts do not change these two distributions.

6. Background Sources

All events containing two muons are a potential source of background for rare dimuonic beauty decays. Of course, the most dangerous are muons originating from B-decays, as they have the same p_T and the same impact

parameter spectrum as muons from rare decays.

The most dangerous background sources have been found to be the following ([23]):

- $B \to \psi X$ decays followed by $\psi \to \mu^+\mu^-$ have the same topology but fixed dimuon masses. These decays can occur at tree level or they are driven by the decay of the Z, W boson or γ in the box and penguin diagrams into a resonant $c\bar{c}$ pair. Their branching ratio is about 10^2 times larger than the branching ratio of rare decays. Only a cut in dimuon invariant mass can remove this background source.$\psi \to \mu^+\mu^-\gamma$ decays are a second order correction to the $\psi \to \mu^+\mu^-$ decays, but they can move out the muons from the ψ window and therefore they have to be take into account as possible background source.
- The $b \to \mu^-\bar{\nu}_\mu c(c \to \mu^+\nu_\mu q)$ semileptonic decay chain, like $B^+ \to \bar{D}^0\mu^+\nu_\mu$ followed by the decay $\bar{D}^0 \to K^+\mu^-\bar{\nu}_\mu$. The two muons seem to come from the same vertex when D does not have a long proper time or when the muon is emitted in the D direction. If the missed mass due to neutrinos is not large, these decays are a very dangerous background source. Vertex requirements and cuts around B-meson mass are the basic tools to reduce this background.
- $b \to \mu\nu_\mu X$ semileptonic decays of both b and $\bar{b}$ quarks. These events are less dangerous than the previous ones to represent a background source as the two muons are not correlated in position.

Other rare semileptonic decays driven by $b \to s\mu^+\mu^-$ transition can be in principle background sources for $B^+ \to K^{(*)+}\mu^+\mu^-$ decays. Their branching ratio is of the same order of magnitude as the two signal channels and their contribution to background is very poor. Same argumentation for the rare decays given by $b \to d\mu^+\mu^-$ transitions: due to CKM matrix element V_{td} the branching ratios of these channels are approximately 10 times smaller than $\mathcal{B}(B^+ \to K^{(*)+}\mu^+\mu^-)$.

Decay	$\mathcal{BR}$
$B \to J/\psi X$ $(J/\psi \to \mu\mu\ (\gamma))$	1.16% (5.88%)
$B \to \psi(2S)X$ $(\psi(2S) \to \mu\mu\ (\gamma))$	4.8×10^{-3} (7.3×10^{-3})
$b \to \mu^-\bar{\nu}_\mu c$ $(c \to \mu^+\nu_\mu q)$	$\sim 1\%$
$b(b) \to \mu\nu_\mu X$	$\sim 1.1\%$

Table 4. *Background sources for $B^+ \to K^{(*)+}\mu^+\mu^-$ decays and their branching ratios.*

6.1. Background Data Samples

The $B \to \psi X$ ($\psi \to \mu\mu$ (γ)), $b \to \mu^- \bar{\nu}_\mu c$ ($c \to \mu^+ \nu_\mu q$) and $b(\bar{b}) \to \mu\nu_\mu X$ decays have been generated together in a so-called $b\bar{b} \to \mu(6GeV)\mu(4GeV)X$ samples. All b and $\bar{b}$ decay channels are left open and accessible in Pythia, but only events containing two muons satisfying the LVL1 trigger cuts are written into a permanent output file.

Two samples of $B^+ \to J/\psi\ K^+$ and $B^+ \to \psi(2S)\ K^+$ with $\psi \to \mu^+\mu^-$ events have been produced including also radiative corrections on ψ decays and LVL1 cuts on muons, in order to evaluate the $c\bar{c}$ resonance width to perform cuts on dimuon invariant mass.

The background sample production is summarized Table 5. Also the number of expected events in 30 fb^{-1} after LVL1 trigger cuts is shown. This number for $b\bar{b} \to \mu(6GeV)\mu(4GeV)X$ events can be computed as

$$N_{b\bar{b}\to\mu(6)\mu(4)X} = \mathcal{L} \cdot t \cdot \sigma_{b\bar{b}\ trig} \tag{4}$$

where $\sigma_{b\bar{b}\ trig} = 3.6 \times 10^{-5} mb$ is the cross section of $b\bar{b}$ events that have the first level trigger as the Pythia output.

Decay	Triggerable events in 30 fb^{-1}	Simulated events
$B^+ \to J/\psi K^+$ ($J/\psi \to \mu^+\mu^-$)	6.2×10^6	5×10^4
$B^+ \to \psi(2S)K^+$ ($\psi(2S) \to \mu^+\mu^-$)	8×10^5	5×10^4
$bb \to \mu(6GeV)\mu(4GeV)X$	1.08×10^9	2.5×10^5

Table 5. *Background sample production with relative expected number of events in* 30 fb^{-1} *after LVL1 trigger cuts on muons.*

6.2. $c\bar{c}$ Resonances

The same analysis strategy for signal reconstruction described in Section 5.2 has been applied on $B^+ \to J/\psi K^+$ and $B^+ \to \psi(2S)K^+$ samples. The goal was to reconstruct the J/ψ and $\psi(2S)$ resonances in order to evaluate their mass width. In Figure 5 the J/ψ and $\psi(2S)$ mass distributions are shown.

Requiring a good dimuon vertex reconstruction ($\chi^2/NDF < 3$), a cut on dimuon invariant mass 3σ around J/ψ and $\psi(2S)$ PDG mass values allows to cut off almost all the events coming from $c\bar{c}$ resonant channels. This is of fundamental importance for the background rejection discussed in the next section.

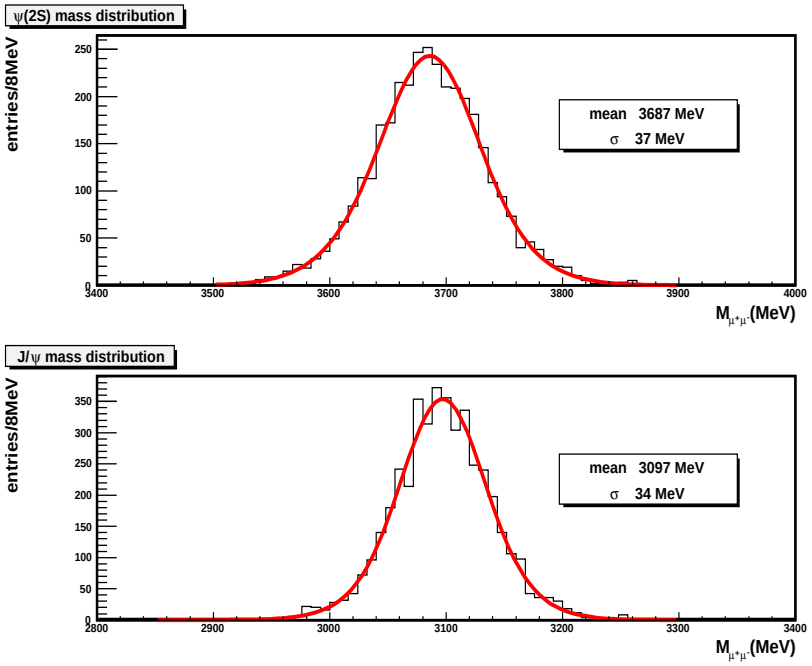

Fig. 5. *J/ψ and $\psi(2S)$ mass distributions: the mean value and the width of the distributions, resulting from a Gaussian fit, are shown.*

7. Background Rejection

The background rejection has been performed using the same analysis code and strategy as the signal reconstruction on $b\bar{b} \rightarrow \mu(6GeV)\mu(4GeV)X$ reconstructed data samples. Cuts on the quantities already identified in the signal reconstruction step have been tuned in order to reduce background efficiency and obtain a signal/background ratio as high as possible. The following two subsections show the background rejection criteria for the two decays.

7.1. $B^+ \rightarrow K^+\mu^+\mu^-$

Dimuon Selection Cuts

As anticipated in Section 6, the muon p_T spectra for background and signal events are similar and no cuts can be applied. Analogous motivations have been adopted for the muon transverse impact parameter.

The dimuon vertex have to be well reconstructed for the ψ resonances rejection: it has been required to have a χ^2/NDF lower than 3.

Figure 6 shows the effect on signal and background dimuon invariant mass normalized distributions[1] after the cut $\pm 3\sigma$ around ψ resonance nominal mass values.

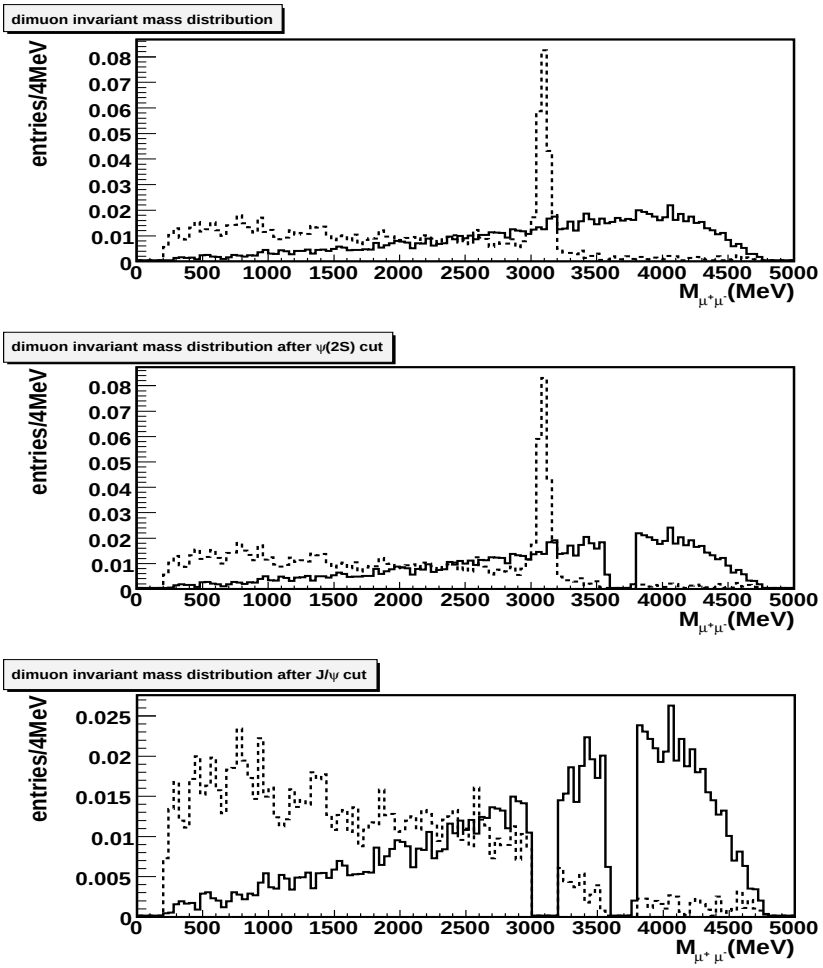

Fig. 6. *Dimuon invariant mass normalized distribution after cuts on ψ resonances for signal (solid line) and background (dotted line).*

Kaon Selection Cuts

A cut on kaon $p_T > 1\ GeV$ remove $\sim 90\%$ of the background yield keeping $\sim 40\%$ of signal events. It has been found the most incisive cut for background rejection.

[1] In the following normalized distribution is intended normalized to 1.

B^+ Selection Cuts

The cuts on B^+ selection are: $\chi^2/NDF < 1.2$, mass in $\pm 3\sigma$ around PDG value and proper time $\tau_{B^+} > 1ps$.

Final Signal and Background efficiencies

A detailed cut description has been reported in Table 6. The final efficiency after the cut application in a sequence for the signal has been found $\varepsilon = 10\%$.Using Eq.2 the number of signal expected events after 30 fb^{-1} integrated luminosity can be determined as:

$$N = \mathcal{L} \cdot t \cdot T \cdot S \cdot \sigma_{b\bar{b}} \cdot P \cdot \mathcal{BR} \cdot \varepsilon \tag{5}$$

leading to 4000 expected events. Due to limited background MonteCarlo statistic, the efficiency for background has been found zero.

Cut	Signal eff.	BG eff.
basic cuts	0.73	0.104
$\chi^2/NDF(dimuon) < 3$	0.92	0.84
$m_{\mu\mu} \notin [m_{\psi(2S)} \pm 3\sigma]$, $\sigma = 37MeV$	0.91	0.99
$m_{\mu\mu} \notin [m_{J/\psi} \pm 3\sigma]$, $\sigma = 34MeV$	0.93	0.79
$p_T(K^+) > 1GeV$	0.37	0.06
$\chi^2/NDF(B^+) < 1.2$	0.28	0.04
$m_{B^+} \in [m_{B^+} \pm 3\sigma]$, $\sigma = 42MeV$	0.49	0.40
$\tau_{B^+} > 1ps$	0.67	0.27
Final efficiency(ε)	0.10	0

Table 6. *Cut description for $B^+ \to K^+\mu^+\mu^-$, efficiency for background rejection and expected events in 30 fb^{-1} of integrated luminosity. The so-called "basic cuts" summarize the vertex fit success requests, the cuts on muon and hadron tracks and dimuon mass in the kinematic allowed window. The original sample was the sample passing the LVL1 trigger requirements.*

7.2. $B^+ \to K^{*+}\mu^+\mu^-$

Dimuon Selection Cuts

Cut on dimuon candidates are the same as those applied for $B^+ \to K^+\mu^+\mu^-$ background rejection (see Section 7.1).

K_s^0 Selection Cuts

A cut on K_s^0 candidate transverse momentum has been added to the cuts on vertex quality and invariant mass. The on K_s^0 selection are $\chi^2/NDF < 10$, mass in $\pm 3\sigma$ around the PDG value and $p_T > 2\ GeV$

K^{*+} Selection Cuts

The cuts on K^{*+} selection are $\chi^2/NDF < 5$, mass in $\pm 3\sigma$ around the PDG value and $p_T > 3\ GeV$

B^+ Selection Cuts

The cuts on B^+ selection are $\chi^2/NDF < 2$, mass in $\pm 3\sigma$ around the PDG value and proper time $\tau_{B^+} > 1\ ps$.

Final Signal and Background efficiencies

A detailed cut description has been reported in Table 7. Also final efficiencies have been tabulated after the cut application in sequence. The final efficiency for signal has been found $\sim 4.5\%$ and this lead to an expected number of event after 30 fb^{-1} integrated luminosity of 2300. As for the $B^+ \to K^+\mu^+\mu^-$ decay, due to limited background MonteCarlo statistic, the efficiency for background has been found zero.

Cut	Signal eff.	BG eff.
basic cuts	0.47	0.25
$\chi^2/NDF(dimuon) < 3$	0.92	0.84
$m_{\mu\mu} \notin [m_{\psi(2S)} \pm 3\sigma]$, $\sigma = 37MeV$	0.94	0.99
$m_{\mu\mu} \notin [m_{J/\psi} \pm 3\sigma]$, $\sigma = 34MeV$	0.93	0.75
$\chi^2/NDF(K^0_s) < 89$	0.89	0.93
$m_{K^0_s} \in [m_{K^0_s} \pm 3\sigma]$, $\sigma = 9MeV$	0.37	0.16
$p_T(K^0_s) > 2GeV$	0.41	0.16
$\chi^2/NDF(K^{*+}) < 5$	0.81	0.87
$m_{K^{*+}} \in [m_{K^{*+}} \pm 3\sigma]$, $\sigma = 26MeV$	0.56	0.46
$p_T(K^{*+}) > 3GeV$	0.43	0.16
$\chi^2/NDF(B^+) < 2$	0.52	0.55
$m_{B^+} \in [m_{B^+} \pm 3\sigma]$, $\sigma = 49MeV$	0.66	0.55
$\tau_{B^+} > 1ps$	0.41	0.15
Final Efficiency(ε)	0.045	0

Table 7. *Cut description for $B^+ \to K^{*+}\mu^+\mu^-$ and efficiency for background rejection. The so-called "basic cuts" summarize the vertex fit success requests, the cuts on muon and hadron tracks and dimuon mass in the kinematic allowed window. The original sample was the sample passing the LVL1 trigger requirements.*

8. Expected Events and Background Estimation

As showed in the previous section, imposing smart cuts allows to remove all the background events coming from beauty decays.

Compatibly whit the current MonteCarlo statistics, an estimate of the background produced in 30 fb^{-1} can be achieved by the following method.

The procedure will be explained in detail for $B^+ \to K^+\mu^+\mu^-$ decay, and then applied also to $B^+ \to K^{*+}\mu^+\mu^-$ channel.

Without applying the cut on B^+ mass, the mass distribution in the range $5000 - 5600\ GeV$ is computed. Counting the events in the mass region, one can obtain the number of background events

$$N_{BG} = 7\ events \tag{6}$$

Looking at the same mass window as the signal i.e. $250\ MeV$, one can compute the number of background events as

$$N_B = rN_{BG} \tag{7}$$

where r is the ratio of the window sizes:

$$r = \frac{250\ MeV}{600\ MeV} \sim 0.42 \tag{8}$$

Clearly the windows sizes and N_{BG} have to be determined using much larger background samples than have been available for this study. With the current statistic, this calculation leads to 2.9 background events within $250\ MeV$. The number of generated events that fulfills the LVL1 trigger is 250000, and it leads to a fake reconstruction efficiency of

$$\varepsilon_{fake} = 1.2 \times 10^{-5} \tag{9}$$

The result leads to a total of $B = \mathcal{L}{\cdot}t{\cdot}\sigma_{b\bar{b}\ trig}{\cdot}\varepsilon_{fake} \sim 12000$ background events in 30 fb^{-1}. In Figure 7 the mass spectrum for background events added to signal events is plotted in the mass range $5000 - 5600\ GeV$. The background is fluctuating around 2400 and on top of it the signal peak is clearly visible.

To test whether the seen peak is a peak and not statistical fluctuation the statistical significance is computed as

$$\mathcal{S}_{stat} = \frac{Signal}{\sqrt{Background}} = \frac{S}{\sqrt{B}} \tag{10}$$

If significance is greater than 5, then the signal is observable. In the analysis with a signal of ~ 4000 events and a background of ~ 12000 events in the signal mass window $m_{B^+} \pm 3\sigma$, a statistical significance of 35 is computed.

For $B^+ \to K^{*+}\mu^+\mu^-$ decay, the same procedure leads to ~ 14000 background events in 30 fb^{-1} in the signal mass window. The statistical significance has been found $\mathcal{S}_{stat} = 19$.

These results are summarized in Table 8.

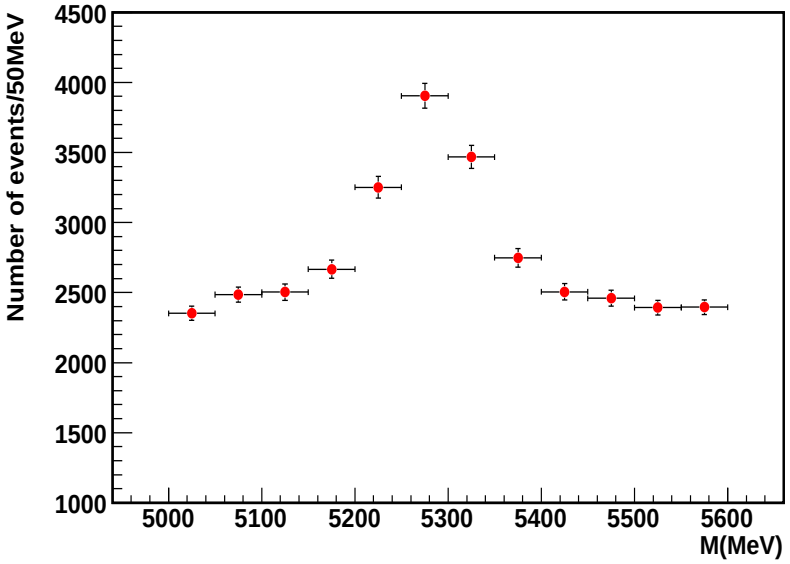

Fig. 7. *The B^+ signal of $B^+ \to K^+\mu^+\mu^-$ decay after 30 fb^{-1} integrated luminosity. The background estimation is done on the available MonteCarlo statistic.*

Decay	ε_i	S_i	B_i
$B^+ \to K^{*+}\mu^+\mu^-$	0.045	2300	14000
$B^+ \to K^+\mu^+\mu^-$	0.10	4000	12000

Table 8. *Expected events for $B^+ \to K^{(*)+}\mu^+\mu^-$ (S_i) and background (B_i) in 30 fb^{-1}. Also the signal efficiency ε_i has been reported.*

9. Branching Ratio Measurements

To estimate the statistical error on an exclusive branching ratio measurement, it has been assumed that in 30 fb^{-1} integrated luminosity $\bar{N}_i$ events are observed in the B^+ mass window, of which $\bar{B}_i$ are background and $\bar{S}_i$ signal events[2]:

[2] Throughout this section X denote the random realization of a variable with mean $\bar{X}$ and following a Poissonian distribution with a large mean, thus $\sigma^2(X) = \bar{X}$.

$$\bar{N}_i = \bar{S}_i + \bar{B}_i \tag{11}$$

The estimates of the signal and background yields are given in table 8.

N_i events are observed in a narrow B mass window and P_i events in a wider window. The background in the narrow mass window is

$$\bar{B}_i = r\bar{P}_i \tag{12}$$

where r is defined as in Eq. (8).

$\bar{S}_i$ will be determined as

$$\bar{S}_i = \bar{N}_i - \bar{B}_i = \bar{N}_i - r\bar{P}_i \tag{13}$$

The numbers of events N_i and P_i observed after 30 fb^{-1} are random realizations of $\bar{N}_i$ and $\bar{P}_i$

$$N_i = \bar{N}_i \pm \sigma(N_i) \qquad \sigma^2(N_i) \sim \bar{N}_i \sim N_i \tag{14}$$

$$P_i = \bar{P}_i \pm \sigma(P_i) \qquad \sigma^2(P_i) \sim \bar{P}_i \sim P_i \tag{15}$$

The statistical error on the number of events S_i is thus given by

$$\sigma^2(S_i) = \sigma^2(N_i) + r^2\sigma^2(P_i) \sim N_i + r^2 P_i \tag{16}$$

In the present case, S_i and B_i are know form the previous section. Using Eq. (11) and (12), Eq. (16) can be rewritten as

$$\sigma^2(S_i) \sim S_i + (1+r)B_i \tag{17}$$

The yield S_i has to be re-weighted by the corresponding selection efficiency ε_i, the generation cuts fraction T and the isospin weight ω_i

$$R_i = \frac{\omega_i}{\varepsilon_i T} S_i = f_i S_i \tag{18}$$

The branching ratio is proportional to R_i, and thus the error is

$$\frac{\sigma(\mathcal{BR}_i)}{\mathcal{BR}_i} = \frac{\sigma(R_i)}{R_i} \tag{19}$$

where $\sigma(R_i) = f_i\sigma(S_i)$. The second term of the uncertainty depending on $\sigma(f_i)$ is not taken into account as it enters the systematic uncertainty.

Using values of ε_i and T given in Table 8 and 2 and 1 and 2.9 as isospin weights respectively for$B^+ \to K^+\mu^+\mu^-$ and $B^+ \to K^{*+}\mu^+\mu^-$ decays, the statistical error on branching ratio for the two decays, is then

$$\frac{\sigma(\mathcal{BR}_i)}{\mathcal{BR}_i}(B^{\pm} \to \mu\mu K^{\pm}) \sim 3.5\% \tag{20}$$

$$\frac{\sigma(\mathcal{BR}_i)}{\mathcal{BR}_i}(B^{\pm} \to \mu\mu K^{*\pm}) \sim 6.5\% \tag{21}$$

The statistical errors are much smaller than the current experimental and theoretical ones. The systematic errors remain to be determined but they are out of scope of this study. These measurements are interesting inputs to test the various theoretical models. They have a potential to be selective between the Standard Model and beyond SM theories.

10. Conclusions

With the present study on the $B^+ \to K^+\mu^+\mu^-$ and $B^+ \to K^{*+}\mu^+\mu^-$ decays, many positive results have been achieved.

All the software chain, from event generation to reconstruction and analysis, has been tested using GRID facilities. The analysis strategy of the two decay channels for the ATLAS data taking is ready. The analysis C++ code has been implemented in the ATLAS official software framework.

The most interesting quantities for the rare semileptonic beauty decays are the differential dimuon invariant mass and the forward-backward asymmetry. New Physics might result in significant enhancement compared to the Standard Model predictions and thus their measurement, as well as the measurement of the branching ratio, provide an indirect search for New Physics. The study on simulated data shows that the trigger and the offline analysis cuts do not change the shape of the dimuon mass spectrum and the FBA distribution.

Also background rejection strategy is ready and it has been tested on $250k$ background events. Due to limited background MonteCarlo statistics, only a preliminary background estimation has been done by extrapolating background events from a wider mass window around PDG B^+ mass value. The signal is clearly visible over the background level: the statistical significance is very high for both decays.

This method leads to an overestimate of the expected background yield. As shown in the ATLAS Technical Design Report ([7]), the expected number of $b\bar{b}$ background events after 30 fb^{-1} for the rare decay $B_d^0 \to K^{*0}\mu^+\mu^-$ is about 300, to be compared with the expected 2000 signal events. But, compatibly with the low MonteCarlo available statistic, this is the only way to demonstrate the visibility of the decays over the background events and to have some prediction on branching ratio measurements. The errors expected on branching ratio measurements are $\sim 3.5\%$ and $\sim 6.5\%$ respectively for

$B^+ \to K^+\mu^+\mu^-$ and $B^+ \to K^{*+}\mu^+\mu^-$ decays. These errors on the branching ratio measurements are much smaller than the current experimental and theoretical ones and this allows to conclude that these measurements are interesting inputs to test the SM versus $SUSY$ theories predicting significant enhancements of these branching ratios.

The present study is being refined by using more MonteCarlo data (background), including also minimum bias pp events and considering pile-up effects to evaluate the possibility to extend the ATLAS studies on rare semileptonic B-decays at high luminosity ($L = 10^{34}\ cm^{-2}s^{-1}$). The contribution of minimum bias events is expected to be poor with respect to the background taken into account, but an accurate estimation of background yield is needed to perform precise measurements of the forward-backward asymmetry and differential decay rate.

REFERENCES

[1] B. Aubert et al. (The BaBar Collaboration), Phys. Rev. **D 73**, 092001 (2006)

[2] A. Ishikawa et al. (The Belle Collaboration), Phys. Rev. Lett. **96**, 251801 (2006)

[3] K. Abe et al. (The Belle Collaboration), hep-ex/0410006 (2004)

[4] G.Buchalla et al., Rev. Mod. Phys.**68**, 1125 (1996)

[5] C. Bobeth et al., Nucl. Phys. **B 574**, 29 (2000)

[6] A.Ali et al., Phys. Rev. **D 66**, 034002 (2002)

[7] ATLAS Collaboration, *ATLAS Detector and Physics Performance Technical Design Report*, CERN/LHCC/99-15 (1999)

[8] S. George, ATL-DAQ-2004-004 (2004)

[9] J. Baines et al., ATL-DAQ-COM-2002-013

[10] M. Smizănská, Eur. Phys J **C 34**, 385-392 (2004)

[11] D. Adams et al., ATL-SOFT-2004-007 (2005)

[12] LCG Project Collaboration, CERN-LHCC-2005-024 (2005)

[13] ATLAS Collaboration, `http://atlas.web.cern.ch/Atlas/GROUPS/SOFTQARE/OO/architecture/General/Tech.Doc/Manual/2.0.0 DRAFT/AthenaUserGuide/pdf`

[14] M. Smizănská, ATL-COM-PHYS-2003-038 (2003)

[15] M. Smizănská and J. Catmore, ATL-COM-PHYS-2004-041 (2004)

[16] S. Baranov and M. Smizănská, ATL-PHYS-98-133 (1998)

[17] W.M. Yao et al., Journal of Physics **G 33**, 1 (2006)

[18] J. Catmore et al., ATL-COM-PHYS-2006-013 (2006)

[19] K.A. Assamagan et al., ATL-SOFT-2004-006 (2004)

[20] http://tarta.home.cern.ch/tarta/vtx/docu.html

[21] D. Fassouliotis et al., ATL-COM-MUON-2003-003 (2003)

[22] J. Baines et al., hep-ph/0003238 (2000)

[23] D. Melikhov et al., *Investigation of rare semimuonic B-decays*, ATL-PHYS-96-083 (1996)